Pergamon

Int. J. Multiphase Flow Vol. 21, No. 5, pp. 851–859, 1995
0301-9322(95)00012-7

0301-9322/95 $9.50 + 0.00

DYNAMICAL ANALYSIS OF PRESSURE-DROP TYPE OSCILLATIONS WITH A PLANAR MODEL

H. T. LIU[1], H. KOÇAK[2] and S. KAKAÇ[1]

[1]Department of Mechanical Engineering, University of Miami, Coral Gables, FL 33124, U.S.A.
[2]Department of Mathematics and Computer Sciences, University of Miami, Coral Gables, FL 33124, U.S.A.

(Received 25 October 1993; in revised form 3 February 1995)

Abstract—A planar system is formulated for pressure-drop type oscillations in a single-channel boiling system, and the pressure-drop type oscillations are analyzed from the perspective of dynamical system theory. The planar system is developed by using a lumped parameter model, in which the system inlet pressure and the mass flow rate are coupled. The results of Hopf bifurcation analysis, the stability criteria and the limit cycles of the pressure-drop type oscillations obtained from the model agree well with experimental results.

Key Words: pressure-drop oscillation, two-phase flow, instability, Hopf bifurcation

1. INTRODUCTION

Boiling two-phase flow systems are prone to several types of flow instabilities, such as density-wave type oscillation, pressure-drop type oscillation, acoustic oscillation, flow excursion and relaxation type instabilities. In the last several decades a considerable amount of research work has been carried out in the field of two-phase flow instabilities, since two-phase flow instabilities can cause serious problems, such as flow-induced structure vibrations, tube thermal fatigue, deterioration of system control. Among the reviews on the work of two-phase flow instabilities are those by Bergles (1981), Yadigaroglu (1981) and Kakaç & Liu (1991).

Pressure-drop type oscillations were first observed by Stenning (1964) and by Maulbetsch & Griffith (1966). Due to the high magnitudes of pressure and mass flow rate fluctuations, and especially the high magnitude of temperature fluctuations they induce in the heater wall, pressure-drop type oscillations are very dangerous once they occur. The analytical proofs have been mostly limited to showing that operation on the negative region of the pressure-drop versus mass flow rate characteristics is unstable in the presence of a compressible volume.

Since experimental results show that the steady-state characteristics curves have two positive slope regions and one negative slope region in between, as mass flow rate continues to increase or decrease, the system should go through two bifurcation points, at one of the points a limit cycle is born and at the other the limit cycle vanishes. Yet theoretical proof of the complete bifurcation diagram is still non-existing. Padki *et al.* (1992) performed the first bifurcation analysis on the pressure-drop type oscillations based on an integral model. The main objective of this study is to prove theoretically the existence, the uniqueness and the stability of the limit-cycle of pressure-drop type oscillations and provide the whole bifurcation diagram of the dynamic system. The model presented here is very simple so that it is easy to capture the main mechanisms of the oscillations, and yet it is not over simplified so that it also gives the whole bifurcation diagram.

2. EXPERIMENTAL INVESTIGATIONS

Figure 1 is a schematic diagram of the two-phase flow loop used in the experimental studies. The test-fluid, R-11, is supplied from the liquid container pressurized by nitrogen gas. The test section is a vertical nichrome tube 60.5 cm long, heated by direct current. Following the test section is a recovery section consisting of a condenser and a collector tank. The mixture of saturated liquid and vapor is led through the condenser coil. The condensed liquid is then stored in a recovery tank

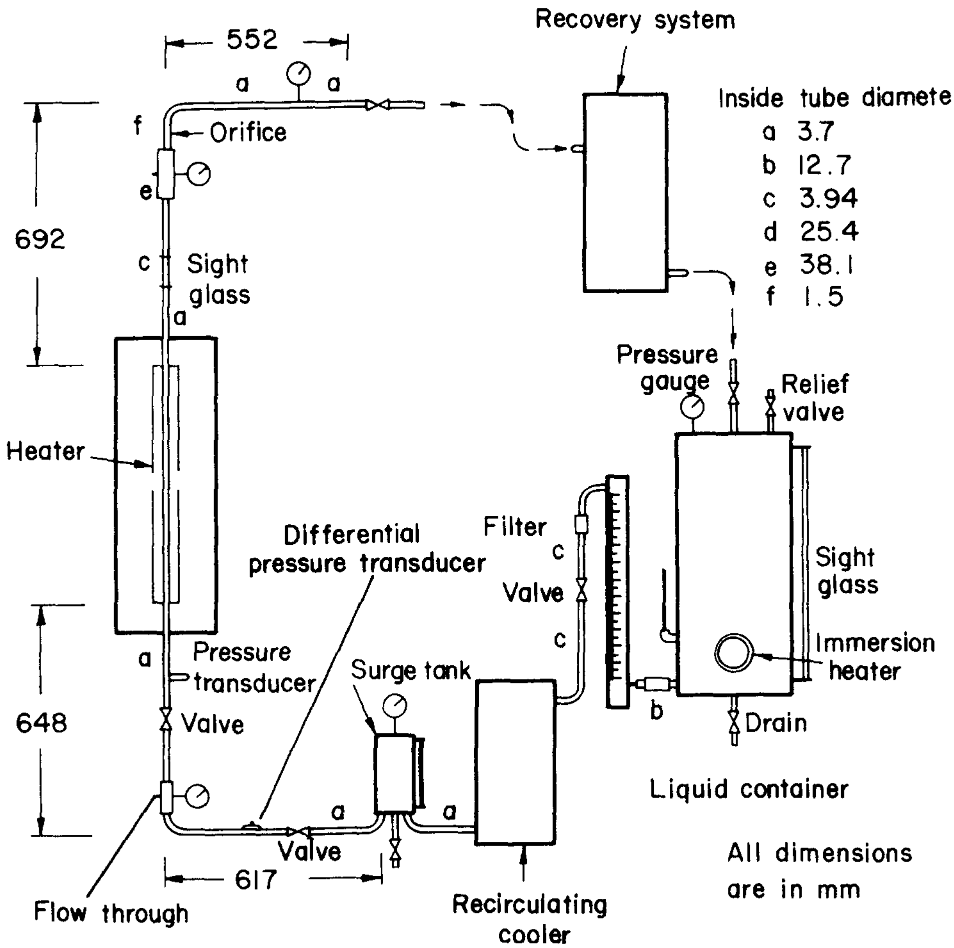

Figure 1. Schematic drawing of the experimental system.

that is maintained at a constant pressure to ensure constant levels of container and exit pressures. The surge tank provides the necessary compressible volume for the pressure-drop oscillations to occur. Appropriate instrumentation is installed to provide control and measurements of the test parameters, namely, flow rate, temperature and pressure at various locations and the electrical heat input. Experimental results and details of the experimental set-up can be found in Liu & Kakaç (1991).

3. THEORETICAL STUDY

3.1. Formulation of the planar model

Figure 2 shows an analytical model of the boiling channel system. The model consists of a feeder section, a heated section and a surge tank upstream of the boiling channel. The steady-state values of the pressure and the compressible volume are P_0 and V_0 respectively. In order to develop the dynamic system equations the following assumptions are made:

(1) The mass flow rate into the surge tank is constant.
(2) At any instant the mass flow rate from the surge tank outlet to the system exit is constant.
(3) The system exit is maintained at constant pressures, P_e.
(4) The temperature inside of the surge tank is constant during oscillations.
(5) The heat input to the fluid is constant.

With these assumptions, the two equations are obtained as follows: the dynamic equation of the surge tank (Akyüzlü *et al.* 1980),

$$\frac{dp}{dt} = p^2 \frac{(M - m)}{(P_o V_o \rho_L)} \qquad [1]$$

and the momentum equation for the test section,

$$\frac{dm}{dt} = \frac{A}{L} [p - P_e - \Delta P(m)] \qquad [2]$$

where p is the surge tank pressure, M is the mass flow rate into the surge tank, P_o is the steady state pressure in the surge tank, V_o is the steady state gas volume in the surge tank, ρ_L is the liquid density in the surge tank, A is the heater inner surface, L is the total test section, P_e is the system exit pressure, ΔP is the system pressure drop and t is time.

At steady state, $m = M$, and a plot of $\Delta P(M)$ versus M is the steady-state characteristics curve. With other parameters specified, $\Delta P(M)$ is a unique function of mass flow rate M. Note that in this experimental system, the pipe diameters from the main tank to the surge tank and to the system exit all have the same diameter.

3.2. *Non-linear simulation of pressure-drop type oscillations*

Once the function form of $\Delta P(m)$ is known, [1] and [2] can be used to simulate the pressure-drop type oscillations. The period of typical pressure-drop type oscillations are much larger than the resident time of fluid particles in the flow; hence the pressure-drop type oscillations are assumed to take place as a succession of quasi-steady-state operating points of the system. Therefore, the steady-state characteristics are used in the simulations. The steady-state characteristics used here are obtained from the experiments. In order to use the discrete experimental data in the simulation, a fourth degree polynomial is obtained by fitting the experimental data. Figure 3 shows the experimental data and the fitted polynomial. A dynamical system simulation software by one of the authors (Koçak 1989) is used to perform the simulations.

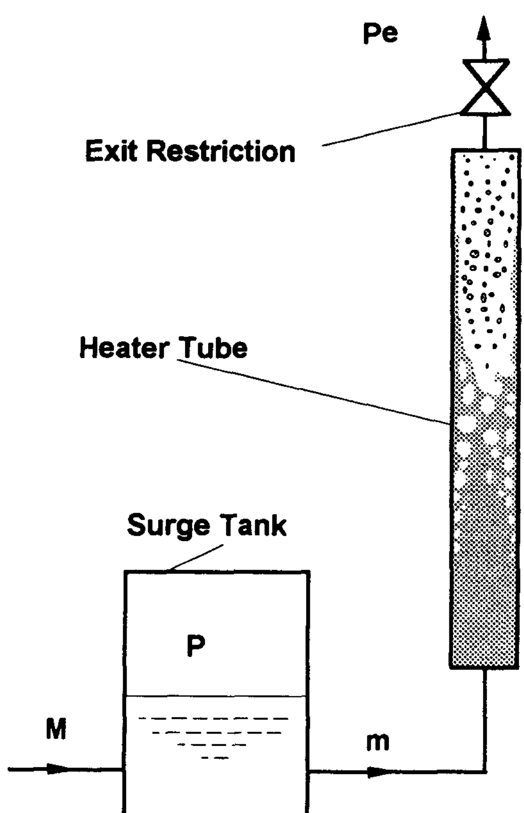

Figure 2. The analytical model of the boiling channel system.

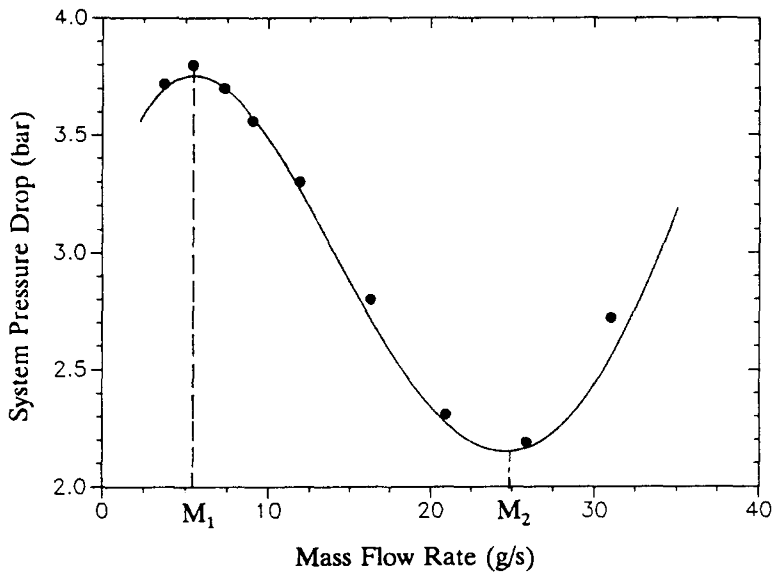

Figure 3. A typical polynomial fitting of the experimental steady-state characteristics used in non-linear simulations. Heat input = 800 W, inlet liquid temperature = 23°C. Heater: coated nichrome, i.d. = 7.5 mm, o.d. = 9.5 mm.

Figure 4 shows a sample of simulation results, along with experimentally obtained recordings. It can be seen that the model gives acceptable results. (The superimposed high-frequency oscillations seen in the experimental results are the density-wave type oscillations. The present model is not designed to simulate these oscillations.)

Figure 5 shows a typical result of how a limit-cycle on the m–p plane is evolved with different initial conditions. It can be seen that no matter what the initial conditions are, the system is always attracted to this periodic attractor, the limit-cycle.

Figure 6 shows a series of simulation results as the mass flow rate increases. The birth, the growth, the decline and the demise of the limit cycle are clearly shown in these figures. These are in agreement with the experimental results: the system is stable when the mass flow rate is small, i.e. in the region where the slope of the steady-state characteristics is positive; the system is unstable when the mass flow rate is medium, i.e. in the region with a negative slope; and the system is stable again when mass flow rate is large, i.e. in the second positive slope region.

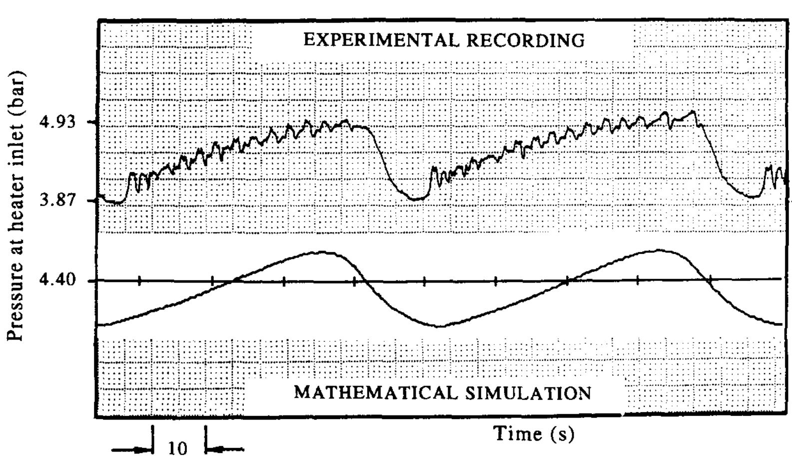

Figure 4. Comparison of non-linear mathematical simulation with experimental recording: inlet pressure oscillations. Heat input = 800 W, inlet liquid temperature = 0°C, inlet mass flow rate = 7.31 g/s. Heater: coated nichrome, i.d. = 7.5 mm, o.d. = 9.5 mm.

The experimental steady-state characteristics are used here in the simulations, but in situations that the experimental data are not available, this model can be used in conjunction with any predicted steady-state characteristics, no matter what two-phase flow model or what two-phase flow pressure drop correlations are used. The more accurate the predictions of the system pressure drop are, the better results the model will produce. This adaptability also gives the model versatility, in addition to its simplicity.

3.3. *Non-dimensionalization of governing equations*

In order to perform stability and bifurcation analysis, it is convenient to shift the equilibrium point of the system to the origin (0, 0). For general applicability, the governing equations need to be in non-dimensional forms. To accomplish these two objectives, we now introduce the following dimensionless parameters,

$$\bar{m} = \frac{m - M}{M} \qquad [3]$$

where $\bar{m}$ is the dimensionless flow rate out of the surge tank,

$$\bar{p} = \frac{p - P_o}{P_o} \qquad [4]$$

where $\bar{p}$ is the dimensionless surge tank pressure,

$$\tau = \frac{t}{V_o \rho_L / M} \qquad [5]$$

where τ is dimensionless time.

Note that $V_o \rho_L / M$ represents the time needed to completely fill the compressible volume V_o at the average mass flow rate M (or inlet mass flow rate).

Substituting [3]–[5] into [1] and [2] the following non-dimensional equations are obtained:

$$\frac{d\bar{p}}{d\tau} = -\bar{m}(\bar{p} + 1)^2 \qquad [6]$$

$$\frac{d\bar{m}}{d\tau} = r \, \mathrm{Eu}[\bar{p} + \Delta\bar{P}(M) - \Delta\bar{P}(M + M\bar{m})] \qquad [7]$$

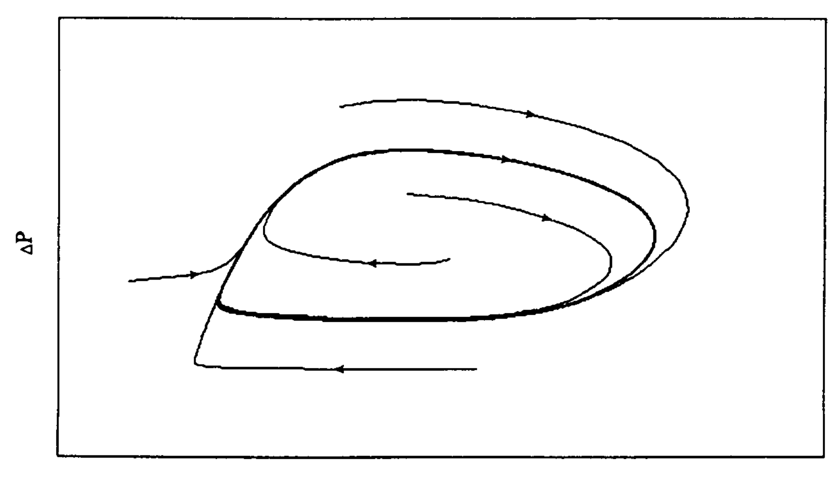

Figure 5. Typical evolutions of a pressure drop type limit-cycle with different initial conditions. Heat input = 800 W, inlet liquid temperature = 23°C, inlet mass flow rate = 15.0 g/s. Heater: coated nichrome, i.d. = 7.5 mm, o.d. = 9.5 mm.

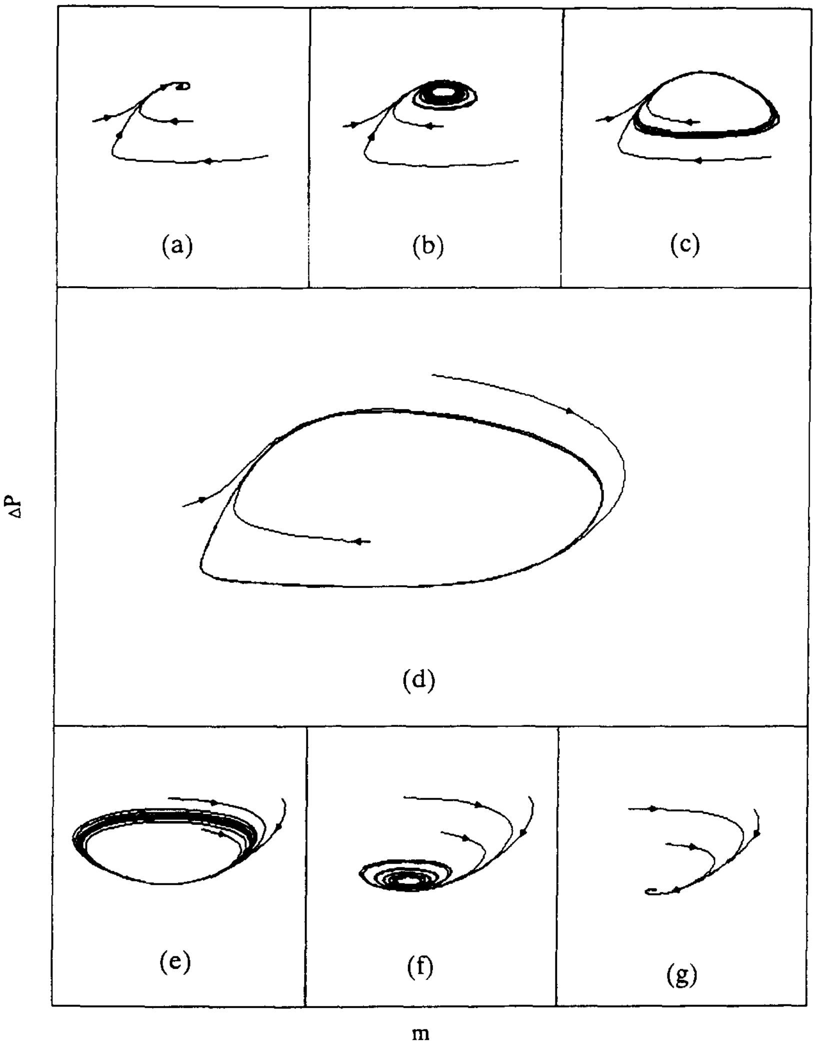

Figure 6. Phase portraits of the planar model with different inlet mass flow rates. (a) $M = 4.0$ g/s, (b) $M = 5.0$ g/s, (c) $M = 5.5$ g/s, (d) $M = 16$ g/s, (e) $M = 24.5$ g/s, (f) $M = 25.0$ g/s and (g) $M = 27$ g/s.

where $\mathrm{Eu} = \Delta P(M)/(M^2/A^2\rho_L)$ is the Euler number, $r = V_o/AL$ is the ratio of surge tank compressible volume to the total inner volume of the test section and $\Delta\bar{P}(\,) = \Delta P(\,)/P_o$, is the dimensionless system pressure drop.

3.4. *Linearized stability analysis*

The system under study has a unique equilibrium point, $\bar{m} = \bar{p} = 0$, for all parameter values. The Jacobian matrix of this system at the equilibrium point is:

$$\mathbf{J} = \begin{bmatrix} -r\,\mathrm{Eu}\,M\dfrac{\partial \Delta\bar{P}(M)}{\partial M} & r\,\mathrm{Eu} \\ -1 & 0 \end{bmatrix} \qquad [8]$$

Note that at the equilibrium point, $m = M$. The characteristic equation for the eigenvalues is,

$$\lambda^2 + e_1\lambda + e_2 = 0 \qquad [9]$$

where,

$$e_1 = r\,\mathrm{Eu}\,M\frac{\partial \Delta\bar{P}(M)}{\partial M} \qquad [10]$$

$$e_2 = r\ \mathrm{Eu} \tag{11}$$

As stated in the stability theorem, the stability of the system of equations is guaranteed when the real parts of both eigenvalues are negative. According to Hurwitz theorem, the necessary and sufficient conditions for the real parts of both eigenvalues to be negative are (Shirer 1987):

(a) $e_1 > 0$, which leads to,

$$\frac{\partial \Delta P(M)}{\partial M} > 0 \tag{12}$$

and

(b) $e_1 e_2 > 0$, which also leads to,

$$\frac{\partial \Delta P(M)}{\partial M} > 0 \tag{13}$$

The two conditions are identical, i.e. a positive slope on the steady-state characteristics. This has been a well-known criterion of stability for pressure-drop type oscillations.

3.5. Bifurcation analysis

Referring to figure 3, it is clear that on a single steady-state characteristics curve there are two points where the slopes are zero. At these points $e_1 = 0$, thus the roots of the characteristic equation are pure imaginary, and the stability type of the equilibrium often changes when subjected to perturbations. These changes in stability types are usually accompanied with either the appearance or disappearance of a small periodic orbit encircling the equilibrium point. To ascertain that the two points with zero slopes are the bifurcation points, we apply the Hopf bifurcation theorem (Hale & Koçak 1991 or Guckenheimer & Holmes 1983).

Choosing M as the bifurcation parameter, we now show that the pair of eigenvalues crosses the imaginary axis with non-zero speed. Differentiating [9] with respect to the bifurcation parameter M at the bifurcation points,

$$\lambda_{1,2} = \pm\sqrt{-e_2} \tag{14}$$

we get,

$$\frac{\partial \lambda_r}{\partial M} = -\frac{2(r\ \mathrm{Eu})^2 M \dfrac{\partial^2 \Delta \bar{P}(M)}{\partial M^2}}{e_1^2 + 4e_2} \tag{15}$$

where λ_r is the real part of an eigenvalue.

At $M = M_1$,

$$\frac{\partial^2 \Delta P(M_1)}{\partial M^2} < 0 \tag{16}$$

So, the pair of eigenvalues crosses the imaginary axis with positive speed. According to Hopf's bifurcation theorem, this indicates the birth of a limit cycle. Therefore, at $M = M_1$, a Hopf bifurcation occurs.

At $M = M_2$,

$$\frac{\partial^2 \Delta P(M_2)}{\partial M^2} > 0 \tag{17}$$

So, the pair of eigenvalues crosses the imaginary axis with negative speed. This indicates the disappearance of the limit cycle. Therefore, at $M = M_2$, a reverse Hopf bifurcation occurs.

It can be shown that the limit-cycle is stable, or the Hopf bifurcations are super-critical. We first rearrange [6] and [7] into the following "standard form":

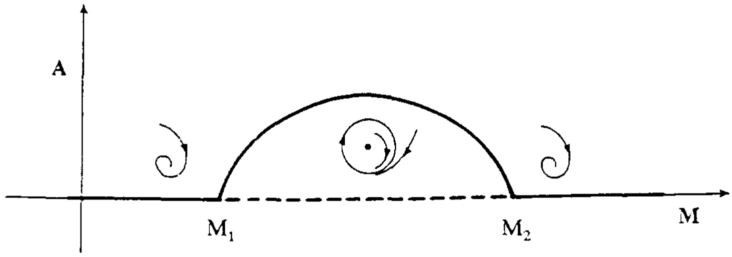

Figure 7. Schematic bifurcation diagram of the planar system: A, the radius of the periodic orbit, which is asymptotically stable, as a function of parameter M.

$$\begin{bmatrix} \dfrac{d\bar{p}}{d\tau} \\ \dfrac{d\bar{m}}{d\tau} \end{bmatrix} = \begin{pmatrix} 0 & -1 \\ 1 & 0 \end{pmatrix} \begin{pmatrix} \bar{p} \\ \bar{m} \end{pmatrix} + \begin{pmatrix} f(\bar{p}, \bar{m}) \\ g(\bar{p}, \bar{m}) \end{pmatrix} \qquad [18]$$

where,

$$f(\bar{p}, \bar{m}) = -\bar{m}(2\bar{p} + \bar{p}^2) \qquad [19]$$

$$g(\bar{p}, \bar{m}) = (r\ \mathrm{Eu} - 1)\bar{p} + r\ \mathrm{Eu}[\Delta\bar{P}(M) - \Delta\bar{P}(M + M\bar{m})] \qquad [20]$$

With $f(0, 0) = g(0, 0) = 0$ and $D[f(0, 0), g(0, 0)] = 0$, the stability of the limit-cycle is determined by the sign of a, where a is given by Guckenheimer & Holmes (1983) as,

$$a = \tfrac{1}{16}[f_{xxx} + f_{xyy} + g_{xxy} + g_{yyy} + f_{xy}(f_{xx} + f_{yy}) - g_{xy}(g_{xx} + g_{yy}) - f_{xx}g_{xx} + f_{yy}g_{yy}] \qquad [21]$$

where $x = \bar{p}$, $y = \bar{m}$ and f_{xy} denotes $\partial f(0, 0)/\partial x\, \partial y$, etc.

If $a < 0$, the Hopf bifurcation is super-critical (the limit-cycle is stable); while if $a > 0$, the Hopf bifurcation is sub-critical (the limit-cycle is unstable).

For the present system, using [21], a is determined to be negative. Therefore, we have showed that the Hopf bifurcations are super-critical.

In conclusion, we have proved that, at $M = M_1$, a super-critical Hopf bifurcation occurs, and at $M = M_2$, a reverse super-critical Hopf bifurcation occurs. This analysis can be shown schematically as the bifurcation diagram in figure 7. When $M < M_1$, the equilibrium point is asymptotically stable; when $M_1 < M < M_2$, the equilibrium is unstable and it gives up its stability to a unique stable limit cycle; when $M > M_2$, the limit cycle contracts to an equilibrium point which is asymptotically stable.

4. CONCLUDING REMARKS

A planar system of equations has been developed based on the experimental set-up and used successfully to predict the stability boundaries, to simulate the pressure-drop type oscillations and to perform bifurcation analysis. The pressure-drop type limit-cycles are generated after super-critical Hopf bifurcation in the two-phase flow dynamic system, and the limit-cycles converge to an asymptotically stable equilibrium point after a reverse supercritical Hopf bifurcation. The dynamic simulations of pressure-drop oscillations and the linear stability analysis based on the planar model compare well with the experimental results.

REFERENCES

Akyüzlü, A., Veziroğlu, T. N., Kakaç, S. & Dogan, T. 1980 Finite difference analysis of two-phase flow pressure-drop and density-wave oscillations. *Wärme Stoffübertr.* **14,** 253–267.

Bergles, A. E. 1981 Instabilities in two-phase system. In *Two-phase Flow and Heat Transfer in the Power and Process Industries* (Edited by Bergles, A. E., Collier, J. G., Delhaye, J. M., Hewitt, G. F. & Mayinger, F.), Chap. 13. Hemisphere McGraw–Hill, New York.

Guckenheimer, J. & Holmes, P. 1983 *Nonlinear Oscillations, Dynamical Systems, and Bifurcations of Vector Fields*, Applied Mathematical Sciences, Vol. 42. Springer, New York.

Hale, J. & Koçak, H. 1991 *Dynamics and Bifurcations*, Texts in Applied Mathematics 3. Springer, New York.

Kakaç, S. & Liu, H. T. 1991 Two-phase flow dynamic instabilities in boiling systems. *Proc. 2nd Int. Symp. on Multi-phase Flow and Heat Transfer* (Edited by Chen, X. J., Veziroglu, T. N. & Tien, C. L.), Vol. 1, pp. 403–444.

Koçak, H. 1989 *Differential and Difference Equations through Computer Experiments*, 2nd edn [with diskettes containing *PHASER: (An Animator/Simulator for Dynamical Systems for I.B.M. Personal Computers)*]. Springer, New York.

Liu, H. T. & Kakaç, S. 1991 An experimental investigation of thermally induced flow instabilities in a convective boiling upflow system. *Wärme Stoffübertr.* **26,** 365–376.

Maulbetsch, J. S. & Griffith, P. 1966 System-induced instabilities in forced-convection flows with subcooled boiling. *Proc. 3rd Int. Heat Transfer Conf.*, Chicago, IL, Vol. 4, pp. 247–257.

Padki, M. M., Palmer, K., Kakaç, S. & Veziroglu, T. N. 1992 Bifurcation analysis of pressure-drop oscillations and the Ledinegg instability. *Int. J. Heat Mass Transfer* **35,** 525–532.

Shirer, H. N. (Ed.) 1987 *Nonlinear Hydrodynamic Modelling: A Mathematical Introduction*, Lecture Notes in Physics, 271, pp. 508–509. Springer, New York.

Stenning, A. H. 1964 Instabilities in the flow of a boiling liquid. *J. Basic Engng, ASME Ser. D* **86,** 213–217.

Yadigaroglu, G. 1981 Two-phase flow instabilities and propagation phenomena. In *Thermal-hydraulics of Two-phase Systems for Industrial Design and Nuclear Engineering* (Edited by Delhaye, J. M., Giot, M. & Riethmuller, M. L.), Chap. 17. Hemisphere McGraw–Hill, New York.